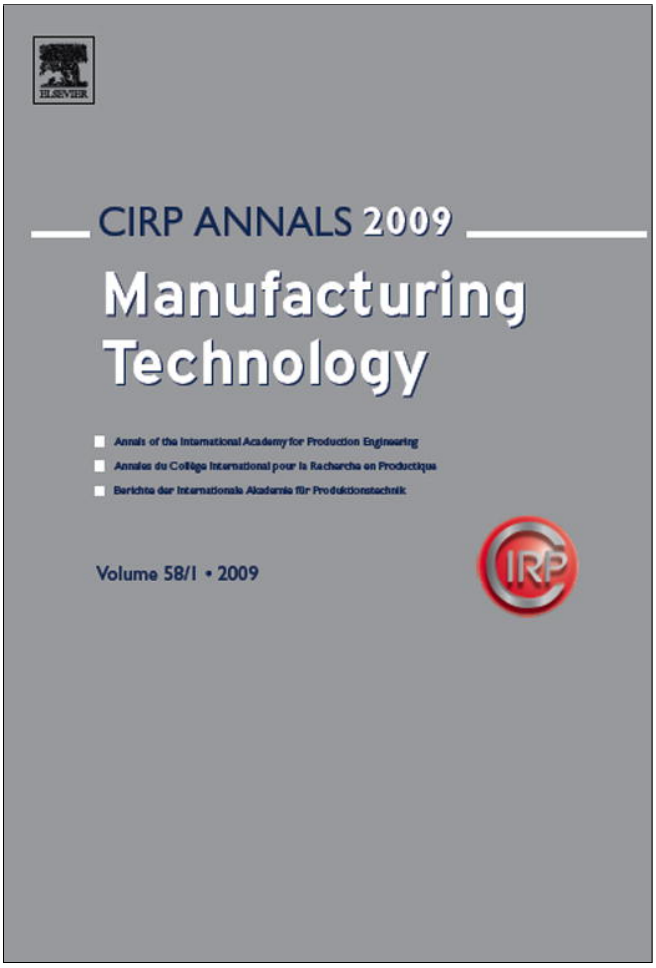
CIRP ANNALS 2009
Manufacturing Technology
Volume 58/1 • 2009

CIRP Annals - Manufacturing Technology 58 (2009) 209–212

Contents lists available at ScienceDirect

CIRP Annals - Manufacturing Technology

journal homepage: http://ees.elsevier.com/cirp/default.asp

# Computational fluid dynamics analysis of working fluid flow and debris movement in wire EDMed kerf

A. Okada (2)[a,*], Y. Uno[a], S. Onoda[a], S. Habib[b]

[a] Department of Mechanical Engineering, Okayama University, Okayama 7008530, Japan
[b] Shoubra Faculty of Engineering, Benha University, Cairo, Egypt

ARTICLE INFO

*Keywords:*
Wire EDM
Flow
Computational fluid dynamics (CFD)

ABSTRACT

In wire EDM, better exclusion of debris from the machined kerf is very important to obtain a stable machining performance. The purpose of this study is to investigate the fluid flow in the kerf and better jet flushing conditions of working fluid from the nozzles. The flow field and the debris motion in the kerf were analyzed by computational fluid dynamics (CFD) simulation, comparing with the observation by high-speed video camera. The influence of flow rate of working fluid from nozzles and the nozzle stand-off distance on flow field in the kerf and debris particle motion were discussed.



## 1. Introduction

The demands for fine precision machining have been recently increased along with the miniaturization of mechanical and electronic products. For meeting these demands, the machine control technology, the optimization of machining conditions and the development of finer electrode have been enhanced in wire EDM. In fine wire EDM using thin electrode, better exclusion of debris from the machined kerf becomes more important in order to obtain a stable machining performance, since the area of spark generation is along a line and much smaller than that in conventional wire EDM using thick wire. When much debris stagnates in the gap and the machined kerf, the secondary discharges possibly occur and the discharges easily concentrate on the same location, which leads to unstable machining performance, wire breakage, low machining rate and low shape accuracy [1–3].

Conventionally, the exclusion of debris is carried out by jet flushing of working fluid from upper and lower nozzles. The purposes are not only flushing away of debris from the spark gap, but also introducing fresh working fluid for dielectric recovery of the gap, and cooling down of electrode and workpiece. As for die sinking EDM, many studies on the fluid flow in the gap and the simulations were done [4–7]. However, for wire EDM, the flow field of working fluid in the machined kerf and the effect of jet flushing conditions from the nozzles have not yet been made clear sufficiently, since such unsteady flow field is not easy to estimate and a precise in-process observation of working fluid flow in the narrow kerf is very difficult. Furthermore, the shapes to be wire EDMed are sometimes complex, and an introduction of effective flow to all gap region is difficult by conventional simple shaped nozzles. The jet flushing with very high flow rate might be effective for complex and thick shapes. However, too high flow rate leads to large wire vibration and bad shape accuracy.

This study aims to investigate the flow field and to obtain better jet flushing conditions of working fluid from the nozzles. The flow field and the debris motion in the kerf were analyzed by computational fluid dynamics (CFD) analysis. The CFD analysis results were compared with the observed results using high-speed video camera to evaluate the accuracy of the CFD analysis results. The debris movement was also estimated by particle tracking analysis. Furthermore, the influences of flow rate from nozzles and the gap between nozzles and workpiece on debris particle motion are discussed.

## 2. High-speed observation

A high-speed observation model of working flow in machined kerf was built to verify the accuracy of CFD analysis results. The system consists of a high-speed video camera, a running thin wire, and a dummy workpiece attached on an observation window, as shown in Fig. 1. The dummy workpiece and the window are made of acrylic so that light can pass through the workpiece wall to obtain a better visual view. On the basis of actual wire EDM for steel of 10 mm in thickness under first cut conditions, the kerf dimensions in the dummy workpiece are decided as follows. The kerf length and width are 10 mm and 0.45 mm, respectively. The side gap distance is 0.125 mm because the diameter of brass wire is 200 μm. Model conditions for high-speed observation are shown in Table 1. In order to obtain a better view of the fluid flow, small amount of vinyl acetate solution is intermittently given to the flow of deionized water from the upper side of kerf.

The recorded movie image of deionized water flow inside the kerf of the dummy workpiece is shown in Fig. 2(a). The black part in the left side is the cross-section of the dummy workpiece and the grey vertical line is the brass wire. The observation area was set to 5.0 mm × 5.0 mm and the recording speed was 500 frames per second (fps). The wire running speed was set to 10 mm/min.

* Corresponding author.

0007-8506/$ – see front matter © 2009 CIRP.
doi:10.1016/j.cirp.2009.03.003

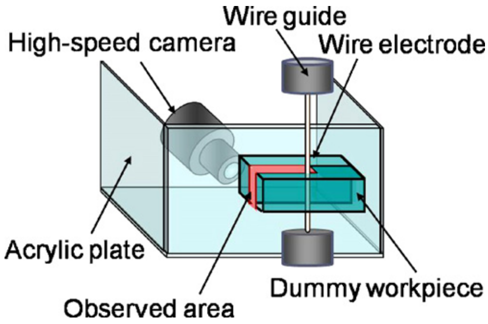


**Fig. 1.** High-speed observation system.

**Table 1**
High-speed observation conditions.

| | |
|---|---|
| Workpiece thickness | 10.0 mm |
| Machining length | 10.0 mm |
| Wire diameter | 0.2 mm |
| Kerf width/side gap | 0.45 mm/0.125 mm |
| Wire running speed | 10.0 m/min |
| Dielectric | Deionized water |
| Fluid's density | 997.561 kg/m$^3$ |
| Viscosity | $8.887 \times 10^{-4}$ Pa s |

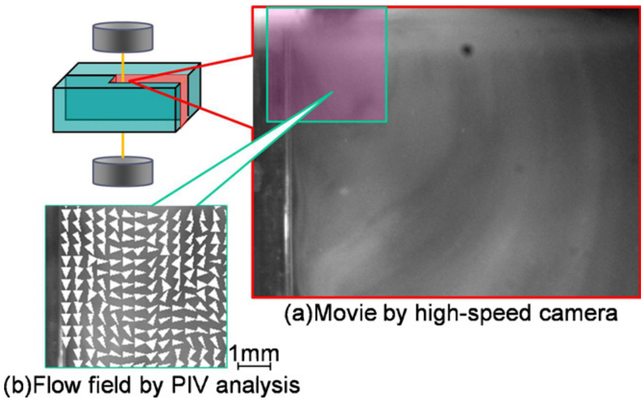


**Fig. 2.** Observed image and PIV analysis results: (a) movie by high-speed camera and (b) flow field by PIV analysis.

Particle Image Velocimetry (PIV) [8] analysis result of the fluid flow image is shown in Fig. 2(b). PIV is a velocity measuring technique using at least two continuous images recorded by high-speed camera. The first image is split into a large number of small shade patches. Thus, the flow field of a fluid can be examined by tracking the movement of each small patch in the next image. In the figure, the arrows represent the direction of the flow at each position and the thickness of arrow indicates the velocity. As shown in the figure, a part of main stream following the wire running from the upper side of workpiece is split into two main flows. One is still following the wire running and the other turns backward and then goes up. The sectional area of main flow into the kerf from upper side of workpiece suddenly becomes very narrow, and so a resistance force acts on the flow going down. Consequently, the turning up flow appears behind the wire.

## 3. CFD analysis

CFD is a revolutionized technique on fluid flow phenomena and some difficult-to-solve problems in fluid dynamics are now possible to be solved with the help of it. The CFD simulations presented in this study are performed with commercial Star-CD. The Star-CD operates by solving the governing differential equations of the flow physics by numerical means on a computational mesh. The governing differential equations are Navier–Stokes equations [9].

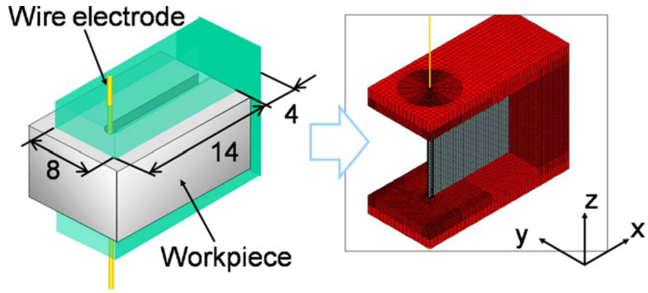


**Fig. 3.** CFD analysis model.

The developed CFD model of wire and machined kerf is schematically illustrated in Fig. 3. The model was three-dimensional and the shapes are equal to the observation model shown above. The cell size adjacent to wire was small enough to simulate precisely, and the other part was a little coarse for saving computational time. The simulations of fluid flow were done by a finite volume method as a three-dimensional, unsteady laminar and turbulent flows [9]. A downward velocity speed of 10 mm/min was given to the circumference surface of wire to realize the actual wire running. Pressure boundary condition was set to a level of 10 mm above the upper surface workpiece. No slip condition was applied to the surfaces of workpiece and wire whereas other boundaries were modeled to be imaginary surface with slip condition. The fluid was deionized water, same as high-speed observation shown above. The effect of gravity, an impact force associated with sparks, electrostatic force acting on wire and wire vibration on the flow were neglected, since CFD analysis with considering them is impossible or very difficult for the current CFD technique. $K$–$\varepsilon$ model with high Reynolds number was chosen for the turbulence model in the simulation of fluid flow using jet flushing from upper and lower nozzles.

The CFD analysis results of flow field generated with wire running in the kerf are compared with the results of PIV analysis at the same area as illustrated in Fig. 4. The area shown in the figure is the upper side of the kerf and the size is 5.0 mm × 5.0 mm. The arrow represents the flow direction and the color is relative velocity. In both analysis results, it can be seen that a part of main stream following the wire running is separated into two main flows. One of them turns backward and then goes upward. Both flow fields are almost the same as each other. Quantitative agreement of them is also confirmed, which indicates very high accuracy of the analyzed results using the CFD model shown above.

## 4. Effect of flow rate of working fluid from nozzles

As shown above, it is proven that the analyzed results using the CFD model has high reliability, since they were quantitatively similar to actual flow fields in wire EDM kerf. Therefore, the effects of flow rate of deionized water from nozzles on flow field in the machined kerf were discussed. Analysis conditions are shown in Table 2.

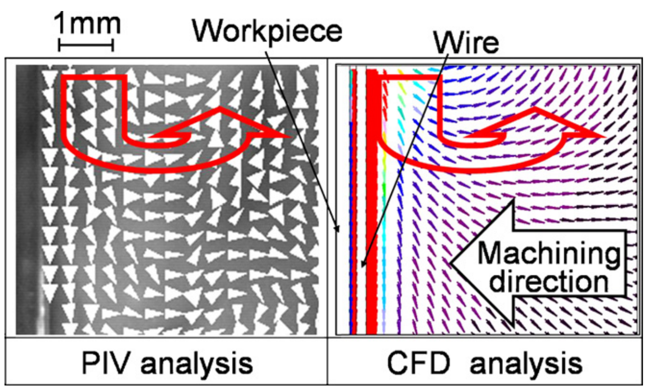


**Fig. 4.** Comparison of PIV and CFD result.

**Table 2**
Fluid flow from nozzle.

| | |
|---|---|
| Nozzle stand-off distance | 2.0 mm |
| Flow rate from nozzles | 1.0, 3.0, 6.0 L/min |
| Nozzles diameter | 6.0 mm |

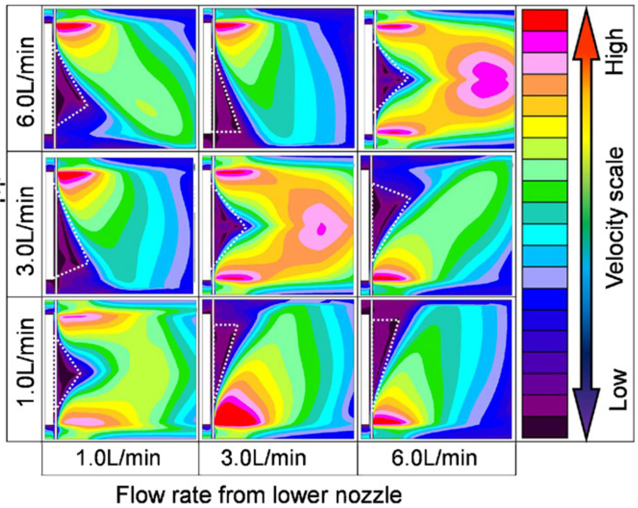


**Fig. 5.** Fluid flow in machined kerf.

In actual wire EDM for workpiece of 10 mm in thickness under first cut condition, the process are done usually with applying jet flushing of working fluid from nozzles in order to well exclude debris generated in the discharge gap. The analysis conditions were decided considering first cut conditions. The stand-off distances from nozzle tips to the upper and lower workpiece surfaces are fixed to 2.0 mm, and the diameter of nozzle is 6.0 mm. In the CFD model, circle inlets of 6 mm in diameter are set at the upper and lower boundary surfaces around the wire, and initial flows in the direction parallel to wire running direction are given.

The flow fields in the machined kerf were analyzed with varying the flow rates of working fluid from upper and lower nozzles are shown in Fig. 5. As can be seen from the figure, a stagnation area where the flow velocity is nearly zero can be confirmed around the center in any flow rate conditions of jet flushing from nozzles. The area is shown as a dotted triangle. This is because the flows from the upper and lower nozzle run against each other. As a matter of course, the exclusion of debris is not efficient in the area. Under any jet flushing conditions, the stagnation area covers most of debris generating area around wire electrode. Therefore, jet flushing of working fluid form upper and lower nozzles is not always effective for exclusion of debris in machined kerf.

## 5. Debris motion

The stability of electrical discharges in the working gap is directly influenced by the debris distribution than flow field of working fluid. When much debris stagnates in the machined kerf, the secondary discharges possibly occur and the discharges easily concentrate on the same location, which leads to unstable machining performance, low machining rate and low shape accuracy. Debris motion in working fluid can be also analyzed by CFD. A Lagrangian/Eulerian kind of framework is used to solve the dispersed two-phase of particle and fluid [10] in the kerf during wire EDM.

Fig. 6 shows the initial location of the debris particles to be tracked. If many debris particles are uniformly distributed in the gap between wire and front machined surface, extremely long time is taken for calculation, and the analyzed results becomes too complex. Therefore, in the present model, eight round particles are uniformly distributed around the wire at 0.16 mm from the wire center on each layer. The tracks of debris on four layers of 0.5 mm,

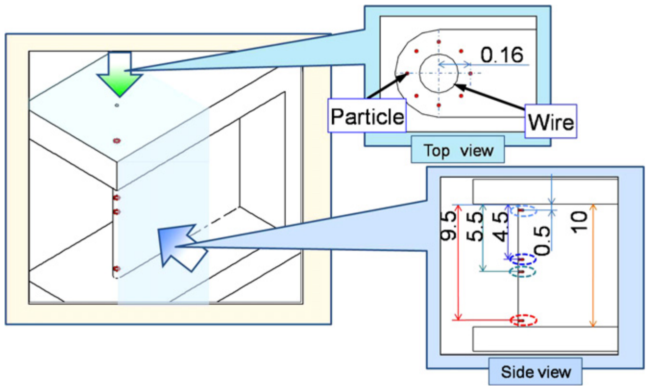


**Fig. 6.** Arrangement of particles.

4.5 mm, 5.5 mm and 9.5 mm form the top edge of workpiece. The colors are light blue, blue, green and red in order from the top. Namely, 32 debris particles are placed. The diameter is 10 μm [11] and the density is 7.8 g/cm$^3$(Fe). In this dispersed two-phase flow model, the influence of gravity is considered, and the momentum transfer process between the two phases is activated so that the motion of the debris will be influenced by the fluid flow. The model also counts for wall bouncing and inter-debris collision.

Fig. 7 shows the analyzed debris tracks with varying the flow rates from upper and lower nozzles. The flow rates from upper and lower nozzles greatly influence debris particle tracks in the machined kerf. Under any flow rate conditions, all debris are excluded out from the same parts of the kerf. For example, when the flow rates from upper and lower nozzles are 3.0 L/min and 6.0 L/min, respectively, all debris goes out from the upper side of the kerf, approximately 10 mm behind the wire. When the flow rate conditions turn upside down, the debris tracks also turn upside down. The debris flowing out position varies with the flow rates from the nozzles. In other words, the position can be controlled by the flow rates from the nozzles. Furthermore, some particles are circulating in the stagnation area with little flow velocity analyzed in Fig. 6. Therefore, it is important to reduce the area for stable wire EDM performance.

Photographs of wire EDMed surface are shown in Fig. 8. A velocity map in the kerf analyzed under the same jet flushing conditions is also shown for comparison. Dark marking can be clearly observed on the wire EDMed surface. On the dark areas, a large quantity of debris is adhered on the surface, which shows that a flow with dense debris passes through the dark parts and/or much debris stagnates. Overlapping of the stagnation area and main stream area of working fluid in the analyzed map almost agree with the dark marking on the surface. Therefore, the debris

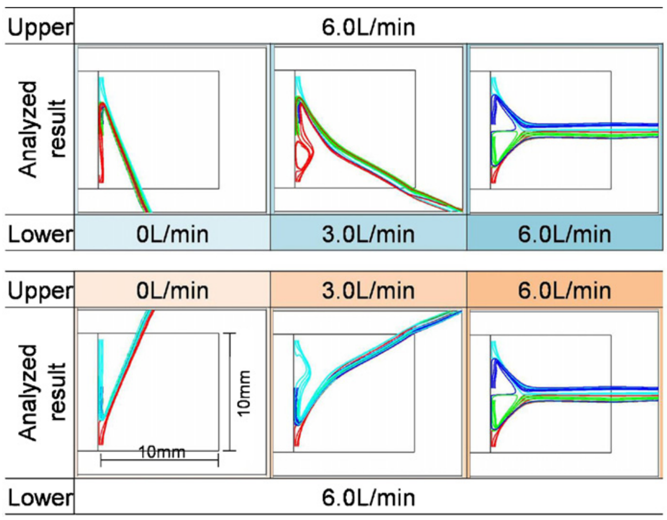


**Fig. 7.** Particle tracks analysis.

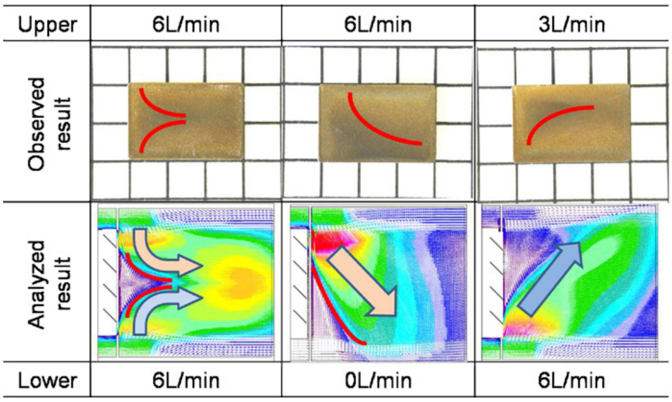


**Fig. 8.** Wire EDMed surfaces and CFD analyzed flow fields.

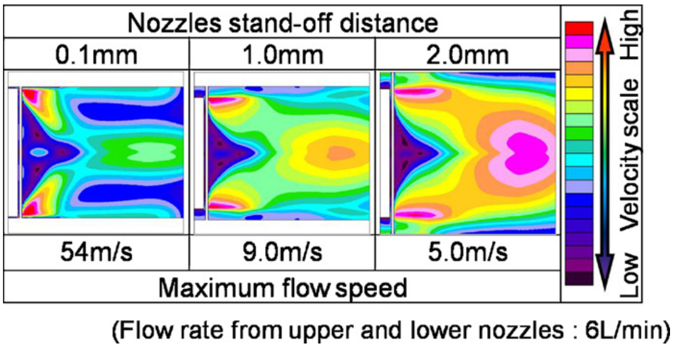


**Fig. 9.** Effect of nozzle stand-off distances.

tracking results analyzed by the model shown in Fig. 6 can well express an actual debris movement. In the analysis, wire vibration, electrostatic force acting on particle, and impact force associated with sparks were not taken into account. However, the analysis results almost agree with the experimental results, thus it is understood that these effects on the debris motion in the kerf can be disregarded in the analysis.

## 6. Effect of nozzle stand-off distance

In practical wire EDM, it is occasionally difficult to arrange the tip of nozzle close to workpiece when the thickness of workpiece is not uniform. At this point, the effect of nozzle stand-off distance on the flow field in the kerf was discussed. When the flow rates from upper and lower nozzles is constantly 6.0 L/min, the flow fields in the kerf were analyzed with varying the upper and lower nozzle stand-off distances. The analyzed results are shown in Fig. 9. The flow velocity in the kerf increases with a decrease of the stand-off distance. However, the stagnation area is almost the same regardless of the nozzle stand-off distance, when the upper distance is equal to the lower distance.

## 7. Conclusions

In this study, the fluid flow and the debris motion in wire EDMed kerf were investigated by CFD simulation comparing with the observation by high-speed video camera. Highly accurate CFD simulation of flow field in wire EDMed kerf could be shown by highly quantitative agreement with the high-speed observation results. The CFD analysis showed that the stagnation area with little flow velocity can be confirmed around the wire under any flow rate conditions of jet flushing from upper and lower nozzles. The exclusion of debris is not efficient in the area, and so jet flushing from upper and lower nozzles is not always effective for debris exclusion in the machined kerf. In addition, debris-tracking analysis clarified that most debris are excluded out from the same parts of the kerf under any constant flow rate conditions. By using the CFD analysis, better jet flushing conditions of working fluid from the nozzles, such as time changing in flow rate, nozzle shape, flushing position, and flushing direction will be analyzed for more effective debris exclusion and high performance wire EDM.

## Acknowledgments

This study was financially supported by Research for Promoting Technological Seeds (No. 12-046), Japan Science and Technology Agency. Okayama prefecture, Japan is also thanked for its support under the Subsidy to Promote Science and Technology.

## References

[1] Koenig W, Weill R, Wertheim R, Jutzler WI (1977) The Flow Fields in the Working Gap with Electro-Discharge-Machining. *Annals of the CIRP* 25(1):71–76.
[2] Schumacher BM (1990) About the Role of Debris in the Gap During Electrical Discharge Machining. *Annals of the CIRP* 39(1):197–199.
[3] Obara H, Abe M, Ohsumi T (1999) Control of Wire Breakage during Wire EDM. *International Journal of Electrical Machining* 4:53–58.
[4] Masuzawa T, Cui X, Taniguchi N (1992) Improved Jet Flushing for EDM. *Annals of the CIRP* 41(1):239–242.
[5] Han F, Kunieda M, Sendai T, Imai Y (2002) High Precision Simulation of WEDM Using Parametric Programming. *Annals of the CIRP* 51(1):165–168.
[6] Cetin S, Okada A, Uno Y (2004) Effect of Debris Accumulation on Machining Speed in EDM. *International Journal of Electrical Machining* 9:9–14.
[7] Takeuchi H, Kunieda M (2007) Effects of Volume Fraction of Bubbles in Discharge Gap on Machining Phenomena of EDM. *Proceedings of 15th ISEM*, 63–68.
[8] Raffel M, Willert CE, Kompenhans J (1998) *Particle Image Velocimetry*. Springer, Berlin.
[9] Wilcox DC (2002) *Turbulence Modeling for CFD*. 2nd ed. DCW Industries, La Canada.
[10] Crove C, Sommerfeld M, Tsuji Y (1998) *Multiphase Flow with Droplets and Particles*. CRC Press, Boca Raton.
[11] Yoshida M, Kunieda M (1998) Study on the Distribution of Scattered Debris Generated by a Single Pulse Discharge in EDM Process. *International Journal of Electrical Machining* 3:39–46.